Intrinsic Limits of Dimensionality and Richness in Random Multipath Fields

Rodney A. Kennedy[†], Parastoo Sadeghi[*], Thushara D. Abhayapala[†], and Haley M. Jones[†]

Research School of Information Sciences and Engineering (RSISE)

The Australian National University

Canberra ACT 0200 Australia

Email: parastoo.sadeghi@rsise.anu.edu.au

Abstract

We study the dimensions or degrees of freedom of farfield multipath that is observed in a limited, source-free region of space. The multipath fields are studied as solutions to the wave equation in an infinite-dimensional vector space. We prove two universal upper bounds on the truncation error of fixed and random multipath fields. A direct consequence of the derived bounds is that both fixed and random multipath fields have an effective finite dimension. For circular and spherical spatial regions, we show that this finite dimension is proportional to the radius and area of the region, respectively. We use the Karhunen-Loeve (KL) expansion of random multipath fields to quantify the notion of multipath richness. The multipath richness is defined as the number of significant eigenvalues in the KL expansion that achieves 99% of the total multipath energy. We prove a lower bound on the largest eigenvalue. This lower bound quantifies, to some extent, the well-known reduction of multipath richness with reducing the angular spread of multipath angular power spectrum. We also provide a numerical algorithm to find multipath eigenvalues, which unlike the Fredholm equation method, does not require selecting quadrature points.

EDICS: SPC-CMOD, SSP-APPL, MSP-CMOD.

Index Terms: Multipath Propagation, Random Scattering, Spatial Correlation Function.

[*]Parastoo Sadeghi is the contact author for this paper.

[†] Thushara Abhayapala and Rodney Kennedy are also associated with the National ICT Australia (NICTA). Haley Jones is now with the Department of Engineering, Faculty of Engineering and Information Technology, The Australian National University, Canberra ACT 0200, Australia.

List of Acronyms

2D	Two-Dimensional
3D	Three-Dimensional
APS	Angular Power Spectrum
KL	Karhunen-Loeve
MSE	Mean Square Error
MMSE	Minimum Mean Square Error
PDE	Partial Differential Equation
SCF	Spatial Correlation Function

I. Introduction

A. Motivation and Background

Wireless communications use *space* as the physical medium for information transfer. The transmitted signal is often received via multiple paths due to reflection, diffraction, and scattering by objects in the wireless environment [1]. Using the spatial aspects of multipath is an increasingly active thread of research in wireless communications and signal processing [2]–[4]. This motivates studying the fundamental physical limits that space imposes on the dynamics of multipath wave propagation and wireless information transfer.

The primary aim of this paper is to find the intrinsic limits on the dimensions or degrees of freedom for multipath fields when they are observed in, or coupled to a source-free region of space. This region of space is where multiple sensors may be potentially located to sample the multipath field for signal processing or communication purposes. However, our aim is to find universal bounds on multipath dimension without explicitly considering a specific sensor setup or application and hence, to show that the coupling of multipath into a spatial region is fundamentally limited by a finite number of orthogonal basis sets or modes.

In this paper we also aim to define spatial multipath richness. The predicted benefits of using spatial multipath in multiple-sensor wireless communications usually hinges on the imprecise assumption of *rich multipath* [5]–[7] or having a rich scattering environment. However, rich

multipath needs to be mathematically quantified based on the dynamics of the multipath field random process and the wave equation. More specifically, we aim to precisely quantify the effects of multipath angular spread and spatial observation region on richness, regardless of sensor setup.

Earlier works, [8], [9] introduced a general theoretical framework for studying the degrees of freedom in spatial multipath fields, where it was proposed that there is an essentially finite number of multipath fields that can be distinctively coupled to a source-free region. In another approach, [10] considered linear, circular, and spherical sensor array geometries and established an analogy between the degrees of freedom in the time-frequency domain and in the spatial-angular domain. It was concluded that the spatial-angular dimensionality is linearly related to the effective sensor array aperture and the angular span of scatterers.

B. Approach

The analysis in this paper considers multipath fields as the *functional* solutions to the wave equation [11]. This mathematical framework is similarly used in [8], [9], [12]. In this presentation, the multipath field lies in a countable infinite-dimensional linear vector space, where vectors consist of functions. The advantage of the functional wave representation is that 1) it is general enough to be applied to *any* narrowband multipath environment, regardless of the number or nature of multipath sources, 2) it accommodates representation of random multipath fields with a general spatial correlation function (SCF) [13], and 3) it allows us to determine the effective number of dimensions (in the infinite-dimensional functional space) that essentially contributes to the coupling of multipath fields to a spatial region. In order not to obscure the approach, we present the main results for a narrowband two-dimensional (2D) multipath farfield environment. We will briefly explain how our methodology extends to three-dimensional (3D) fields. Unless explicitly stated, the equations and results in the paper are written assuming 2D multipath fields.

The integral kernels for spatial channel response in [10] and multipath field representations in this paper are both derived from solutions to Maxwell equations. As a result, the integral kernels in [10] for circular and spherical antenna arrays are based on similar orthonormal expansions as in 2D and 3D multipath fields in this paper, respectively. One difference is that [10] considers a *zoomed-out* granularity for describing channel scattering, where the total effect of scattering is modeled by the angular power span in the kernels. In this paper, scattering is directly incorporated into

the multipath field representation using a countable set of random coefficients. These coefficients encode the field and characterize the statistical details of angular power spectrum[1] (APS). Another difference is that [10] takes antenna polarization into account and shows that using tri-polarized arrays can result in a maximum two-fold increase in multipath channel dimensionality. In this paper, we focus on uni-polarized representation of multipath, where a similar conclusion as in [10] is expected by including polarization.

It is known that the Karhunen-Loeve (KL) expansion [14] of a random process allows a parsimonious representation/truncation of the process in the minimum mean square error (MMSE) sense. The KL expansion of a non-isotropic multipath field provides the maximally parsimonious and customized orthonormal expansion for that particular field. Therefore, we propose to use the KL expansion of random multipath fields to quantify their richness. In the KL expansion of multipath fields, the SCF eigenvalues and eigenfunctions play a central role. In particular, the number of significant SCF eigenvalues defines multipath richness, since random multipath is essentially generated by the corresponding significant eigenfunctions and an uncorrelated random sequence.

C. Contributions

The Dimension of Multipath Fields: In Section III, we prove two universal upper bounds on the truncation error of multipath fields in their infinite-dimensional presentation to a finite number of orthogonal modes. The first upper bound considers fixed multipath fields and complements the preliminary results in [8] by providing a mathematically rigorous proof. The second upper bound explicitly considers random multipath fields and upper bounds the field truncation mean square error (MSE). We show that for 2D multipath fields, the truncation (mean square) error upper bound exponentially decays to zero, if the number of considered orthogonal modes is greater than a critical number $2N+1$. The critical value N is directly related to the normalized radius of the 2D region R/λ and is given as $N \triangleq \lceil \pi\, R\, e\, /\, \lambda \rceil$ ($\lceil \cdot \rceil$ is the integer ceiling function and λ is the wavelength). The results are noteworthy, as they show that the dimensionality in fixed or random 2D multipath fields is essentially limited by the *radius* and not by the *area* of the 2D observation/coupling region.

[1]The angular power spectrum quantifies the distribution of multipath power from different incident angles.

The dimensionality in 3D multipath fields is determined by $(N+1)^2$ and hence, is related to the *area* and not the *volume* of the 3D region.

Multipath Richness: In Section IV, we use the multipath KL expansion to quantify the notion of multipath richness based on the number of significant SCF eigenvalues. More specifically, richness is defined as the number of SCF eigenvalues that captures at least 99% percent of the total multipath energy. This definition provides multipath richness results that are consistent with the $2\lceil \Omega\, R\, e\, /\, \lambda \rceil + 1$ definition in [12], where Ω is the APS angular power spread. In [10], the channel dimensionality using uni-polarized, 2D circular arrays was shown to be $A|\Omega|$, for $R \gg 1$, where $A = 2R/\lambda$ is the normalized array aperture and $|\Omega|$ is the solid angular spread of scatterers. We also prove a lower bound on the largest SCF eigenvalue. This lower bound quantifies, to some extent, the well-known qualitative effect of decreasing angular power spread of scatterers on decreasing multipath richness. We also provide a systematic numerical algorithm to find the SCF eigenvalues. Unlike the quadrature-based solution to the Fredholm equation [15], [16], the proposed algorithm does not require selecting quadrature points.

II. 2D Multipath Field Representation

Let $\boldsymbol{x}$ represent a vector in 2D space, $\mathbb{R}^2$, and let $r = \|\boldsymbol{x}\|$ denote the Euclidean distance of $\boldsymbol{x}$ from the origin, which is the center of some region of interest. The unit vector in the direction of non-zero vector $\boldsymbol{x}$ is denoted $\widehat{\boldsymbol{x}} \triangleq \boldsymbol{x}/\|\boldsymbol{x}\|$. Further, let $\varphi(\boldsymbol{x}) \in [0, 2\pi)$ represent the azimuth angle of vector $\boldsymbol{x}$. Then, we can write $\widehat{\boldsymbol{x}} = [\cos\varphi(\boldsymbol{x}), \sin\varphi(\boldsymbol{x})]^T$, where T denotes transpose. The vector $\boldsymbol{x}$ may also be represented in its polar form as

$$\boldsymbol{x} \equiv (\|\boldsymbol{x}\|, \varphi(\boldsymbol{x})) \equiv (r, \varphi).$$

Let $F(\boldsymbol{x})$ denote a finite complex-valued narrowband multipath field in a region of interest $\|\boldsymbol{x}\| \leqslant R$, for some finite range R, generated by sources and scatterers *external* to that region.[2] In particular, we assume that all sources exist outside some radius $R_s > R$. Then, $F(\boldsymbol{x})$ satisfies the Helmholtz or reduced wave equation (in the region of interest) [11]

$$\triangle F(\boldsymbol{x}) + k^2 F(\boldsymbol{x}) = 0, \quad k \triangleq 2\pi/\lambda, \quad \|\boldsymbol{x}\| \leqslant R, \tag{1}$$

[2]More generally the region could be any shape. This paper considers circular regions, because this is one of the cases where rigorous analytic bounds are possible. How more general shapes can be treated in an analogous way is not explicitly treated in this paper.

where $\triangle$ is the Laplacian and λ is the wavelength. The time harmonic solution to the related full wave equation is then $F(\boldsymbol{x},t) = F(\boldsymbol{x})\, e^{-i\omega t}$, where $i = \sqrt{-1}$, $\omega = 2\pi f$, and f is the frequency [11]. Since (1) is a linear partial differential equation (PDE), we see immediately that valid multipath fields in a source-free region of interest are constrained to lie in a linear subspace given by the nullspace of the operator $M \triangleq \triangle + k^2 I$ (I is identity). That is, if F_1 and F_2 are any two solutions of (1), then so is $\zeta_1 F_1 + \zeta_2 F_2$ with ζ_1 and ζ_2 being scalars.

Two broad classes of representation of the solution to (1) will be considered. The first class is based on plane wave synthesis and is considered in Section II-A. The second class is based on orthogonal solutions to the wave equation and is considered in Section II-B.

A. Multiple Plane Wave Representation

A standard multipath model involves modeling every distinct path explicitly as a plane wave. That is,

$$F(\boldsymbol{x}) = \sum_p a_p\, e^{ik\boldsymbol{x}\cdot\widehat{\boldsymbol{y}}_p}, \tag{2}$$

where the plane wave of index p has complex amplitude $a_p \in \mathbb{C}$, the propagation direction is denoted by the unit vector $\widehat{\boldsymbol{y}}_p \equiv (1, \varphi_p)$, and $\boldsymbol{x}\cdot\boldsymbol{y}$ denotes the scalar product between vectors $\boldsymbol{x}$ and $\boldsymbol{y}$. We interpret representation (2) as encoding the field with a countable number of pairs $\{a_p, \widehat{\boldsymbol{y}}_p\}$ enumerated by p. Representations similar to (2) appear in array sensor signal processing applications, such as in [17]. Typically, only a finite number of plane waves are considered, although distributed sources are considered in [18]–[20]. For example, [20] extended the classical Bello's work [21] and established the duality between continuous spatial direction dispersion and spatial selectivity. The spatial duality is analogous to the duality between delay dispersion and frequency selectivity or between Doppler frequency dispersion and time selectivity in wireless channels.

A ready generalization that subsumes (2) is the superposition of plane waves from all azimuth directions φ as

$$F(\boldsymbol{x}) = \int_0^{2\pi} a(\varphi)\, e^{ik\boldsymbol{x}\cdot\widehat{\boldsymbol{y}}}\, d\varphi, \tag{3}$$

where $\widehat{\boldsymbol{y}} \equiv (1, \varphi)$ and $a(\varphi)$ is the complex-valued gain of scatterers as a function of the direction of arrival φ.

B. Orthogonal Representation

A more general representation than (3), which implicitly required that any sources be in the farfield, is now given. If we assume that the narrowband multipath field is generated by sources outside some radius R_s, then for $R_s \to \infty$, we can use the Jacobi-Anger expansion [11, p. 67] to represent the plane waves in (3) as

$$e^{ik\boldsymbol{x}\cdot\widehat{\boldsymbol{y}}} = \sum_{n=-\infty}^{\infty} i^n \, J_n\big(k\|\boldsymbol{x}\|\big) \, e^{in(\varphi(\boldsymbol{x})-\varphi)}, \tag{4}$$

where $J_n(\cdot)$ is the Bessel function of the first kind of integer order n [22], [23]. By substituting (4) into (3), we obtain

$$F(\boldsymbol{x}) = \sum_{n=-\infty}^{\infty} i^n \, \alpha_n \, J_n\big(k\|\boldsymbol{x}\|\big) \, e^{in\varphi(\boldsymbol{x})}, \quad \|\boldsymbol{x}\| \leqslant R < R_s, \tag{5}$$

where $\alpha_n \in \mathbb{C}$ is the n^{th} Fourier series coefficient of $a(\varphi)$ in (3) defined as

$$\alpha_n = \int_0^{2\pi} a(\varphi) \, e^{-in\varphi} \, d\varphi, \tag{6}$$

and

$$a(\varphi) = \sum_{n=-\infty}^{\infty} \frac{\alpha_n}{2\pi} \, e^{in\varphi}. \tag{7}$$

This shows the relationship between the angular distribution of farfield sources $a(\cdot)$ in (3) and the coefficients $\{\alpha_n\}$ of the general expression (5). In (5), we identify a countable set of orthonormal basis functions over the 2D disc of size R as

$$\Phi_n(\boldsymbol{x}) \triangleq i^n \, \frac{J_n\big(k\|\boldsymbol{x}\|\big)}{\sqrt{\mathcal{J}_n(R)}} \, \frac{e^{in\varphi(\boldsymbol{x})}}{\sqrt{2\pi}}, \quad n \in \mathbb{Z}, \quad \|\boldsymbol{x}\| \leqslant R. \tag{8}$$

where

$$\mathcal{J}_n(R) \triangleq \int_0^R J_n^2(kr) r dr. \tag{9}$$

The orthonormality is verified

$$\int_0^R \int_0^{2\pi} \Phi_n(\boldsymbol{x}) \Phi_m^*(\boldsymbol{x}) d\varphi r dr = \begin{cases} 1 & m = n \\ 0 & \text{otherwise} \end{cases}. \tag{10}$$

We can rewrite (5) in its orthonormal expansion

$$F(\boldsymbol{x}) = \sum_{n=-\infty}^{\infty} \sqrt{2\pi \mathcal{J}_n(R)} \alpha_n \, \Phi_n(\boldsymbol{x}). \tag{11}$$

In comparison with (2) and (3), representation (11) encodes the field with a countable set of Fourier coefficients $\{\alpha_n\}_{n\in\mathbb{Z}}$. Moreover, the multipath field in (11) is represented as a superposition of a countable set of orthonormal basis functions $\{\Phi_n(\boldsymbol{x})\}_{n\in\mathbb{Z}}$, whereas (2) lacks a parsimonious property, since plane waves lack orthogonality.

The sequence $\{\alpha_n\}_{n\in\mathbb{Z}}$ in (5) and its statistical properties play a central role in this paper, as they provide, through truncation, an efficient or parsimonious parameterization of general narrowband multipath fields and allow studying their dimensionality or degrees of freedom.

C. Random Multipath Fields

Detailed information about scatterers that generate the multipath field $F(\boldsymbol{x})$ is usually limited. Therefore, it is reasonable to represent multipath field $F(\boldsymbol{x})$ as a random process. Referring to (3), the scattering gain $a(\cdot)$ is random and so is α_n in (11). For mathematical tractability of the analysis, we assume uncorrelated scattering, which means that the random gains $a(\varphi)$ and $a(\varphi')$ at two distinct incident angles are uncorrelated from each other and the normalized APS is given by

$$P(\varphi) \triangleq \frac{\mathcal{E}\left\{a(\varphi)\, a^*(\varphi)\right\}}{\int_0^{2\pi} \mathcal{E}\left\{a(\varphi)\, a^*(\varphi)\right\} d\varphi}, \tag{12}$$

where $\mathcal{E}\{\cdot\}$ and $*$ denote expectation and complex conjugate, respectively. Using (6), (12), the uncorrelated scattering assumption, and following a few intermediate steps we find that

$$\mathcal{E}\big\{|\alpha_n|^2\big\} \;=\; \int_0^{2\pi} \mathcal{E}\big\{a(\varphi)a^*(\varphi)\big\} d\varphi. \tag{13}$$

The normalized correlation between α_n and α_m is defined as

$$\gamma_{m-n} \triangleq \frac{\mathcal{E}\left\{\alpha_m\, \alpha_n^*\right\}}{\mathcal{E}\big\{|\alpha_n|^2\big\}} = \int_0^{2\pi} P(\varphi)\, e^{-i\,(m-n)\,\varphi}\, d\varphi. \tag{14}$$

It is observed from (14) that γ_{m-n} is, in fact, the $(m-n)^{th}$ Fourier series coefficient of the normalized APS, $P(\varphi)$.

Using (3), the normalized spatial correlation function (SCF) of multipath fields $F(\boldsymbol{x}_1)$ and $F(\boldsymbol{x}_2)$ at points $\boldsymbol{x}_1$ and $\boldsymbol{x}_2$ is defined as [13]

$$\rho(\boldsymbol{x}_2, \boldsymbol{x}_1) = \frac{\mathcal{E}\left\{F(\boldsymbol{x}_2)F^*(\boldsymbol{x}_1)\right\}}{\mathcal{E}\left\{F(\boldsymbol{x}_1)F^*(\boldsymbol{x}_1)\right\}} \tag{15}$$

$$= \frac{\int_0^{2\pi}\int_0^{2\pi} \mathcal{E}\big\{a(\varphi)a^*(\varphi')\big\}\, e^{ik\,\boldsymbol{x}_2.\widehat{\boldsymbol{y}}}\, e^{-ik\,\boldsymbol{x}_1.\widehat{\boldsymbol{y}'}}\, d\varphi d\varphi'}{\int_0^{2\pi}\int_0^{2\pi} \mathcal{E}\big\{a(\varphi)a^*(\varphi')\big\}\, e^{ik\,\boldsymbol{x}_1.\widehat{\boldsymbol{y}}}\, e^{-ik\,\boldsymbol{x}_1.\widehat{\boldsymbol{y}'}}\, d\varphi d\varphi'}. \tag{16}$$

Since we assume uncorrelated scattering, $\mathcal{E}\{a(\varphi)a^*(\varphi')\}$ in (16) is only non-zero for $\varphi = \varphi'$. Therefore, the double integrals in (16) reduce to single integrals and upon using the APS definition in (12), $\rho(\boldsymbol{x}_2, \boldsymbol{x}_1)$ is simplified to

$$\rho(\boldsymbol{x}_2, \boldsymbol{x}_1) = \rho(\boldsymbol{x}_2 - \boldsymbol{x}_1) = \int_0^{2\pi} P(\varphi) e^{ik\,(\boldsymbol{x}_2 - \boldsymbol{x}_1).\widehat{\boldsymbol{y}}}\, d\varphi. \tag{17}$$

Equation (17) shows that due to the uncorrelated scattering assumption, the SCF is only a function of the spatial separation between points $(\boldsymbol{x}_2 - \boldsymbol{x}_1)$ and therefore, is spatially stationary. Using the Jacobi-Anger expansion (4) for the plane waves in (17) yields

$$\rho(\boldsymbol{x}_2 - \boldsymbol{x}_1) = \sum_{m=-\infty}^{\infty} i^{-m} J_m(k\|\boldsymbol{x}_1\|)\, e^{-im\varphi(\boldsymbol{x}_1)} \sum_{n=-\infty}^{\infty} i^n \gamma_{n-m}\, J_n(k\|\boldsymbol{x}_2\|)\, e^{in\varphi(\boldsymbol{x}_2)} \tag{18}$$

$$= \sum_{m=-\infty}^{\infty} i^m \gamma_m J_m(k\|\boldsymbol{x}_2 - \boldsymbol{x}_1\|)\, e^{-im\varphi_{21}}, \tag{19}$$

where the second equality is written using the summation theorem for Bessel functions [24, pp. 930-931]. In (19), $\|\boldsymbol{x}_2 - \boldsymbol{x}_1\|$ is the distance between vectors $\boldsymbol{x}_2$ and $\boldsymbol{x}_1$ and φ_{21} is the angle of the vector that connects $\boldsymbol{x}_1$ to $\boldsymbol{x}_2$. The SCF in (17)-(19) will be used later in Section III-B and Section IV to find the dimensionality and richness of random multipath fields, respectively.

Before concluding this section, we reiterate that the assumption of spatially uncorrelated scattering, originally used in [21] for uncorrelated scattering in delay dispersion domain, enables a mathematically tractable analysis. However, the assumption of spatially uncorrelated scattering may be violated in practical situations, where electromagnetic rays reflect non-specularly off scatterers and the received amplitudes and phases of paths with similar angles of arrivals become correlated. Recently, [25] proposed a physical model to represent spatially correlated scattering, which requires a two-dimensional Fourier expansion of the scattering APS, $P(\varphi)$. It is shown that a scattering correlation with Gaussian density and the standard deviation of 2 degrees has modest and mostly negligible effects on the SCF, whereas for a randomly generated angular correlation, the difference cannot be neglected. The actual effect of correlated scattering on the dimensionality of multipath fields is still unknown. Our conjecture is that it could only reduce the dimensionality and not increase it. Hence, the results of this paper may serve as an upper bound on the available degrees of freedom. Quantifying the effects of correlated scattering on multipath dimensionality is an open problem.

III. Dimensionality of Multipath Fields

Multipath fields are usually observed in a limited region in space and, as such, the degree to which one can determine the effects of the multipath field is also limited. In the following sections, we will see that one needs to consider explicitly the region in space when considering concepts such as dimension and richness.

In Section II-B, the multipath field $F(\boldsymbol{x})$ was represented by a countable, but infinite sum of orthogonal modes $\{\alpha_n \Phi_n(\boldsymbol{x})\}$ in (11). In this section, we define the dimensionality of multipath by the number or cardinality of effective modes that essentially build the field. To this end, we define the *truncated* field $F_N(\boldsymbol{x})$ by selecting the first $2N+1$ indexed coefficients of $F(\boldsymbol{x})$

$$F_N(\boldsymbol{x}) \triangleq \sum_{n=-N}^{N} \sqrt{2\pi \mathcal{J}_n(R)} \alpha_n \Phi_n(\boldsymbol{x}). \tag{20}$$

As will be shown in the following sections, although all α_n coefficients in the synthesis of multipath field in (11) have the same variance (refer to (13)), it is still possible to accurately truncate the field with a carefully chosen truncation length, N. Equivalently, the truncated field in (20) is synthesized as if the Fourier coefficients α_n were zero for $|n| > N$. The question is how to choose N so that the truncated field represents the actual field $F(\boldsymbol{x})$ within a given region and with a prescribed accuracy.

Our approach consists of two parts. In Section III-A, we find an upper bound on the normalized truncation error of the multipath field as a function of the truncation length N. This is carried out for an arbitrary multipath (subject to satisfying conditions discussed in Section II), without explicitly considering its random nature. Hence, the field is assumed to be deterministic. From the truncation error upper bound in Section III-A we conclude that the effective dimensionality of multipath is directly related to the radius of the 2D region, to which the field is coupled. Then in Section III-B, we find a universal upper bound on the normalized MSE of multipath field truncation, which takes multipath randomness into account. Considering the truncation MSE upper bound consistently predicts the same dimensionality for random multipath fields as in Section III-A. This is expected, because the absolute upper bound in Section III-A applies for *any* multipath. However, the MSE upper bound bears a more physical significance, because 1) it takes the stochastic random scattering into account by computing the average error and 2) it signifies the normalized *energy* of truncation error, which is more physically meaningful than the absolute error. Moreover,

considering truncation MSE of random multipath fields paves the way for the MMSE KL expansion of multipath in Section IV and for investigating the dimensionality of random fields with a limited angle of arrival and quantifying multipath richness.

A. Arbitrary, Deterministic Multipath Fields

Using (11) and (20), we define the normalized field truncation error of the multipath field over a 2D disk of radius R

$$\varepsilon_N(R) \triangleq \frac{1}{\pi R^2} \int_0^R \int_0^{2\pi} \frac{\big|F(\boldsymbol{x}) - F_N(\boldsymbol{x})\big|}{\|a\|} d\varphi r dr, \tag{21}$$

where, assuming farfield sources $R_s \to \infty$, $\|a\|$ is finite and defined to be

$$\|a\| \triangleq \int_0^{2\pi} |a(\varphi)|\, d\varphi < \infty. \tag{22}$$

Based on (22) and referring to (3), the field intensity $|F(\boldsymbol{x})|$ is also upper bounded by $\|a\|$. The normalization in (21) provides a relative error satisfying properties of: i) scale invariance, that the relative error is the same for $F(\boldsymbol{x})$ and $\gamma F(\boldsymbol{x})$ for complex scalar $\gamma \neq 0$; and ii) unit plane wave invariance, that normalization leaves a unit amplitude plane wave unchanged.

We now elaborate on the normalized truncation error in (21) in two steps. First, we show that the two fields $F(\boldsymbol{x})$ and $F_N(\boldsymbol{x})$ are essentially indistinguishable at any point $\|\boldsymbol{x}\| \leqslant R$, provided that N is appropriately chosen according to $\|\boldsymbol{x}\|$. More specifically, we show that the normalized field residual

$$\frac{\big|F(\boldsymbol{x}) - F_N(\boldsymbol{x})\big|}{\|a\|} \to 0$$

in an exponential manner for $N > \lceil e\,\pi \|\boldsymbol{x}\|/\lambda \rceil$, $\lceil \cdot \rceil$ being the integer ceiling function. This is formally expressed in Theorem 1. Then, it is shown that the decaying property of truncation error carries over to a 2D disk of size R. In particular, the truncation error in (21) exponentially approaches zero for $N_R > \lceil e\,\pi R/\lambda \rceil$.

Now, consider the integrand in (21), which is written using (5)

$$\begin{aligned} \zeta_N(\boldsymbol{x}) \triangleq \frac{\big|F(\boldsymbol{x}) - F_N(\boldsymbol{x})\big|}{\|a\|} &= \frac{1}{\|a\|} \Big| \sum_{|n|>N} i^n \alpha_n\, J_n\big(k\|\boldsymbol{x}\|\big)\, e^{in\varphi(\boldsymbol{x})} \Big| \\ &\leqslant \frac{1}{\|a\|} \sum_{|n|>N} |\alpha_n|\, |J_n(kr)| \\ &\leqslant \sum_{|n|>N} |J_n(kr)| \;=\; 2 \sum_{n>N} |J_n(kr)|, \end{aligned} \tag{23}$$

where the second inequality follows from (6) and (22) $\big(|\alpha_n| \leqslant \|a\|\big)$ and the last equality follows from $J_{-n}(kr) = (-1)^n J_n(kr)$. From (23) it is evident that the behavior of the truncation error depends on the properties of Bessel functions $|J_n(kr)|$ for sufficiently large n. We use the following bound for the Bessel function $|J_n(u)|$ [26, p. 362]

$$|J_n(u)| \leqslant \frac{(u)^n}{2^n n!}, \qquad z \geqslant 0 \tag{24}$$

to upper bound (23) as

$$\zeta_N(\boldsymbol{x}) \leqslant 2 \sum_{n>N} |J_n(kr)| \leqslant 2 \sum_{n>N} \frac{(kr)^n}{2^n n!}. \tag{25}$$

The following theorem shows quantitatively that, for a fixed $\boldsymbol{x}$, by taking the truncation depth N large enough, we can make $\zeta_N(\boldsymbol{x})$ as small as desired.

***Theorem** 1 (**Relative Truncation Error Bound of the Multipath Field**): A multipath field $F(\boldsymbol{x})$ generated by farfield sources, having representation* (11)*, can be truncated to $|n| \leqslant N$ terms as in* (20)*, where the normalized truncation error is upper bounded as*

$$\zeta_N(\boldsymbol{x}) \triangleq \frac{\big|F(\boldsymbol{x}) - F_N(\boldsymbol{x})\big|}{\|a\|} \leqslant \eta\, e^{-\Delta}, \tag{26}$$

provided that the truncation length is chosen as

$$N = \lceil e\,\pi \|\boldsymbol{x}\|/\lambda \rceil + \Delta. \tag{27}$$

In the above, $\eta \approx 0.16127$ and $\Delta \in \mathbb{Z}^+$.$\square$

Theorem 1 states that the relative truncation error is no more than 16.1% once N equals the critical threshold $\lceil e\,\pi\|\boldsymbol{x}\|/\lambda\rceil$, and thereafter decreases at least exponentially to zero as N increases. See Appendix I for the proof.

Now, we turn back to the definition of the normalized truncation error (21) over a disk of radius R. We note that $\zeta_N(\boldsymbol{x})$ in (25) only depends on $r = \|\boldsymbol{x}\| \leqslant R$. From Theorem 1 we conclude that for a fixed r, ζ_N is a decreasing function of $N > \lceil e\,\pi r/\lambda\rceil$. Therefore, we choose $N_R = \lceil e\,\pi\, R/\lambda\rceil + \Delta$, so that the truncation error at the outer edge of disc is bounded as $\zeta_{N_R}(r = R) \leqslant \eta\, e^{-\Delta}$. Since $N_R \geqslant \lceil e\,\pi r/\lambda\rceil$ for every $r \leqslant R$, $\zeta_N \leqslant \eta\, e^{-\Delta}$ for every $r \leqslant R$. As a result, $N_R = \lceil e\,\pi\, R/\lambda\rceil + \Delta$ guarantees $\varepsilon_N(R) < \eta\, e^{-\Delta}$ over the entire region. This is summarized in the following corollary to Theorem 1.

Corollary 1.1 (Truncation of Multipath Fields in a 2D Region): *A multipath field $F(\boldsymbol{x})$ may be truncated to $F_N(\boldsymbol{x})$ as in* (20) *in the region $\|\boldsymbol{x}\| \leqslant R$ whenever N_R equals (or exceeds)*

$$N_R \triangleq \lceil e\,\pi\,R/\lambda \rceil, \tag{28}$$

with a normalized truncation error given in (21) that is exponentially decaying to zero for $N > N_R$.

Theorem 1 complements the preliminary results in [8] by explicitly quantifying how the normalized truncation error ζ_N in (26) exponentially decreases as a function of excess truncation length Δ, and by providing a more rigorous and detailed mathematical derivation of the bound in Appendix I. More specifically, in [8] the normalized truncation error ζ_N was bounded as

$$\zeta_N(\boldsymbol{x}) \leqslant \sqrt{\frac{2}{(N+1)\pi}}.\frac{\rho(N,\|\boldsymbol{x}\|)^{N+1}}{1-\rho(N,\|\boldsymbol{x}\|)}, \tag{29}$$

where

$$\rho(N,\|\boldsymbol{x}\|) = \frac{\pi e\|\boldsymbol{x}\|/\lambda}{N+1}, \tag{30}$$

and $N > \pi e\|\boldsymbol{x}\|/\lambda - 1$. Equation (29) does not explicitly elaborate on how $\zeta_N(\boldsymbol{x})$ behaves for $N = \lceil e\,\pi\|\boldsymbol{x}\|/\lambda\rceil + \Delta$. Quantifying the truncation error $\zeta_N(\boldsymbol{x})$ in the form of (26) is one contribution of this paper. Corollary 1.1 is an another contribution of this paper, compared to [8], which explicitly defines and upper bounds the normalized truncation error over a 2D disk of radius R.

Example: Fig. 1 compares the predicted relative truncation error bound in Theorem 1 with multipath simulation results. We have synthesized a large number of 2D multipath fields according to the plane wave model (2) and computed and plotted the worst case relative error $\max_{\|\boldsymbol{x}\|\leqslant R}\{\zeta_N(\boldsymbol{x})\}$ in (23) over the circular region $\|\boldsymbol{x}\| \leqslant 1\,\lambda$ (λ is the wavelength). The parameter is the truncation depth N. Note that in the context of an antenna array for communications, this region is not so small since, for example, it would accommodate a linear array of 5 antennas or 13 antennas in a diamond configuration at $\lambda/2$ spacing. Fig. 1 summarizes the results of 50 trials, each of fields composed of $P \in \{1, 2, 5, 10, 50, 100, 200, 500, 1000\}$ numbers of plane waves. The complex amplitude, a_p, of each plane wave was randomly selected from a uniform $[0, 1]$ amplitude distribution, uniform $[0, 2\pi)$ phase distribution, and uniform $[0, 2\pi)$ direction of propagation φ_p. It is evident that for all fields, the relative error decreases faster than exponentially with increasing N. In this figure we have also plotted the bound (26). According to Theorem 1 and (28), for a 2D region of size

$\|\boldsymbol{x}\| \leqslant 1\,\lambda$ the truncation error exponentially decays if $N = N_R + \Delta = \lceil \pi\, e \rceil + \Delta \geqslant 9$. It is evident that the relative error bound is quite conservative and the actual relative error is of the order of 1% at $N_R = 9$ (in comparison to our bound of approximately 16.1%). The bound exponent does, however, well model the slope of the relative error at $N \approxeq N_R$. The fact that the slope is greater at higher truncation lengths can be inferred in the proof given in Appendix I (see (68b)), but has not been reflected in Theorem 1 to simplify its statement. These experiments and similar experiments for regions of different sizes verify that one can bound the relative error *independent of the multipath field* where the bound *depends only on the size of the region*. Therefore, it is essentially impossible to distinguish between fields with relatively few paths and ones with 1000 or more paths (including diffuse multipath) for this size region. This example quantitatively confirms the well-known limitation that array aperture (size) imposes on resolving multipath fields.

B. Random Multipath Fields

In this section, we prove a universal bound on the truncation error of random multipath fields in the MSE sense. Since the multipath field is a random process, we compute the normalized truncation MSE over a 2D disc with radius R, when the field in (11) is truncated to its first $2N+1$ terms in (20). This is defined as

$$\overline{\varepsilon}_N(R) = \frac{\int_0^R \int_0^{2\pi} \mathcal{E}\big\{\big|F(\boldsymbol{x}) - F_N(\boldsymbol{x})\big|^2\big\}\, d\phi\, r\, dr}{\int_0^R \int_0^{2\pi} \mathcal{E}\big\{\big|F(\boldsymbol{x})\big|^2\big\}\, d\phi\, r\, dr}. \tag{31}$$

Since Theorem 1 and Corollary 1.1 already showed that multipath truncation to $2N+1$ terms is possible for *any* deterministic field, we expect that considering truncation MSE provides a consistent conclusion about the choice of N. However, the MSE truncation error defined in (31) is physically more meaningful than (21), because it evaluates the normalized average energy of error. As will be seen in Theorem 2, the truncation MSE upper bound decays even faster than (26) with excess truncation length Δ and hence, strengthens the physical significance of the results. We use (11), (20), the orthonormality of basis functions $\Phi_n(\boldsymbol{x})$ in (10), and the definition of $\mathcal{J}_n(R)$ in (9) to write the MSE in (31) as

$$\overline{\varepsilon}_N(R) = \frac{\int_0^R \sum_{|n|>N} \mathcal{E}\{\big|\alpha_n\big|^2\} J_n^2(kr) r\, dr}{\int_0^R \sum_n \mathcal{E}\{\big|\alpha_n\big|^2\} J_n^2(kr) r\, dr}. \tag{32}$$

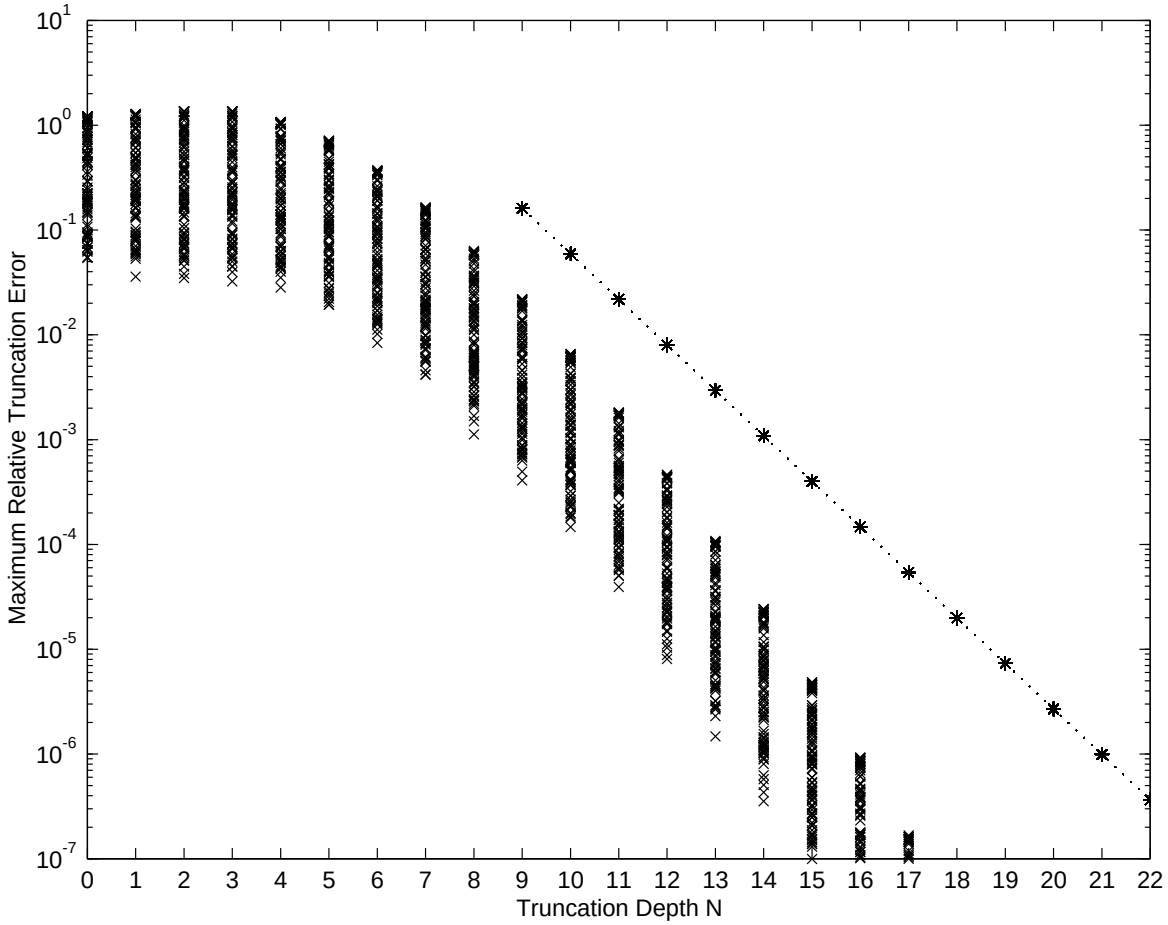

Fig. 1. Simulation results for the maximum relative error $\max_{\|\boldsymbol{x}\|\leqslant R}\{\zeta_N(\boldsymbol{x})\}$ versus the truncation order N for a circular 2D region, $\|\boldsymbol{x}\| \leqslant 1\,\lambda$, for a large number of randomly generated 2D multipath fields. Every trial value is marked with a cross. The stars define the analytic bound of (26) for $N = N_R + \Delta = \lceil \pi\, e \rceil + \Delta \geqslant 9$, which is independent of the multipath field.

From (13) it is observed that the expectation $\mathcal{E}\{\big|\alpha_n\big|^2\}$ is independent of index n, which yields

$$\bar{\varepsilon}_N(R) = \frac{\int_0^R \sum_{|n|>N} J_n^2(kr) r\, dr}{\int_0^R \underbrace{\sum_n J_n^2(kr)}_{1}\, r\, dr} = \frac{\int_0^R \sum_{|n|>N} J_n^2(kr) r\, dr}{(1/2)R^2}, \tag{33}$$

where the summation in the denominator is equal to 1 according to the summation theorem for Bessel functions [24, pp. 930-931]. To find an upper bound for (33), we use the same bound for the Bessel functions given in (24). The following theorem provides a universal upper bound for the MSE in (33).

Theorem** 2 **(Universal MSE Upper Bound for Truncation of 2D Random Multipath Fields):

A random multipath field $F(\boldsymbol{x})$ generated by farfield sources, having representation (11)*, can be truncated to $|n| \leqslant N$ terms as in* (20)*, with the normalized truncation MSE given in* (33) *upper bounded as*

$$\overline{\varepsilon}_N(R) \leqslant \sigma\, e^{-2\Delta}, \tag{34}$$

provided that N is chosen as $N = \lceil e\pi R/\lambda \rceil + \Delta$ and $\Delta \in \mathbb{Z}^+$. In (34)*, $\sigma = 0.0093$.*$\square$

The proof is provided in Appendix II. We note that in the derivation of multipath truncation MSE in (31)-(34), we did not assume anything about the multipath SCF $\rho(\boldsymbol{x}_2 - \boldsymbol{x}_1)$ or equivalently the APS $P(\phi)$ in (17). Therefore, (34) is a universal bound on multipath truncation MSE, regardless of multipath scattering spatial correlation. Therefore, no matter how *random* the scatter is, the field can be truncated to $2N+1$ terms in (20) with an exponentially decaying MSE given in (34). In other words, $2N+1$ is an upper bound on the effective richness of random multipath fields in the MSE sense.

So far, we have observed that the truncation of multipath fields results in an exponentially decaying error both in the absolute and MSE sense for the truncation depth $N \geqslant \lceil e\pi R/\lambda \rceil$ (Theorems 1 and 2), where the actual number of terms in (20) to represent the field is $2N+1$. As was observed in Fig. 1, the above truncation length is quite conservative. We are now in a position to provide the following definition for the dimension of multipath fields.

***Definition** 1 (**Universal Bound on the Dimension of 2D Random Multipath Fields**): For a circular region in space given by $\|\boldsymbol{x}\| \leqslant R$, the effective dimension of a 2D multipath field is given by*

$$\mathcal{D}_R^{\text{2D}} \triangleq 2\lceil e\,\pi\, R/\lambda \rceil + 1 \approx \lceil 17.079\, R/\lambda \rceil + 1. \tag{35}$$

Here, we summarize a few observations based on the above definition.

- The dimension, $\mathcal{D}_R^{\text{2D}}$ increases with the *linear size* of the region R/λ (in wavelengths), not with the area of the region.
- The dimension increases with the precision required. Dimension (35) actually specifies a *threshold effect* where the truncation error is small (in the sense of Theorems 1 and 2 and Corollary 1.1) and is decreasing with an exponential rate.

- It is sufficient to use only $\mathcal{D}_R^{\text{2D}}$ of the α_n in (11) to effectively encode any field within a distance R of the origin.

In the following two subsections we interpret the finite dimensionality of multipath fields in the context of spatial sampling and multiple antenna communication systems.

C. Spatial Sampling

If an actual multipath field $F(\boldsymbol{x})$ can be expressed exactly in the form (20) for some N, then we refer to the multipath field as being *mode-limited*. Hence we have an exact sampling theory analogous to the sampling theory of time harmonic functions. That is, $2N+1$ appropriately chosen sampling points in space are sufficient to completely determine $F(\boldsymbol{x})$ in the 2D region.

For a general field $F(\boldsymbol{x})$ restricted to the region $\|\boldsymbol{x}\| \leqslant R$, our theory implies that $F(\boldsymbol{x})$ is *essentially* mode-limited within $\|\boldsymbol{x}\| \leqslant R$ and, thereby, is well represented by a limited number of spatial samples (equal to the dimension). The point to be made is that a sufficiently regular multipath field[3] has an *intrinsic* spatial forgetting which gives it a natural parsimonious representation in terms of the lower order terms in the expansion (11).

D. Numbers of Receiver Antennas

We can interpret the finite dimensionality of multipath fields in the context of multiple antenna communication systems. Consider Q antennas in a region $\|\boldsymbol{x}\| \leqslant R$ at distinct locations $\boldsymbol{x}_1$, $\boldsymbol{x}_2$, $\ldots$, $\boldsymbol{x}_Q$ that are sampling a multipath field $F(\boldsymbol{x})$ for communication purposes, such as multiple-input multiple-output (MIMO) systems [3], [4]. Since $F(\boldsymbol{x})$ is well-modeled by $F_N(\boldsymbol{x})$ with $\mathcal{D}_R^{\text{2D}}$ terms given in (35), we can regard up to $Q - \mathcal{D}_R^{\text{2D}}$ of the antennas as superfluous – that is, any number of antennas in the region $\|\boldsymbol{x}\| \leqslant R$ beyond the dimension of the region, $\mathcal{D}_R^{\text{2D}}$, provide little or no additional information, depending on how wisely the antennas are spaced. *This guides how densely we can usefully populate space with antennas. For small spatial regions $\mathcal{D}_R^{\text{2D}}$ is small and the asymptotic analysis and predictions about MIMO capacity enhancements should be cautiously interpreted.*

[3]Sufficiently regular in the sense of this paper means the multipath field is generated by discrete or distributed farfield sources. The generalization to nearfield sources requires a more refined argument which is beyond the scope of this paper, but nonetheless the general conclusion remains.

E. Extension to 3D Multipath Fields

After studying the dimensionality of 2D multipath fields, we are interested to find how the results are extended to the 3D case. For this purpose one needs to consider the 3D equivalent of the 2D Helmholtz equation in (1) for a spherical region of radius R/λ wavelengths, or $\|\boldsymbol{x}\| \leqslant R$. The solution to 3D Helmholtz equation is more mathematically involved than (5) and is given by

$$F(\boldsymbol{x}) = 4\pi \sum_{n=0}^{\infty} i^n \, j_n\big(k\|\boldsymbol{x}\|\big) \sum_{m=-n}^{n} \alpha_n^m \, Y_n^m(\widehat{\boldsymbol{x}}), \;\; \|\boldsymbol{x}\| \leqslant R, \tag{36}$$

where $\alpha_n^m \in \mathbb{C}$ are constants independent of position, and

$$j_n(z) \triangleq \sqrt{\frac{\pi}{2z}} J_{n+1/2}(z) \tag{37}$$

are the spherical Bessel functions, and

$$Y_n^m(\widehat{\boldsymbol{x}}) \triangleq \sqrt{\frac{2n+1}{4\pi} \frac{(n-|m|)!}{(n+|m|)!}} \, P_n^{|m|}(\cos\theta) \, e^{im\varphi} \tag{38}$$

are the spherical harmonic functions, which are expressed in terms of the associated Legendre polynomials $P_n^m(\cos\theta)$. In (38), θ is the elevation angle and φ is the azimuth angle, as before. The 3D field in (36) is encoded with the countable set $\{\alpha_n^m\}$, which are 3D counterparts of α_n in (5). Also, Y_n^m and Y_q^p are orthogonal for $m \neq p$ or $n \neq q$. It was shown in [27] that the first summation in (36) can be truncated to N terms as

$$F_N(\boldsymbol{x}) = 4\pi \sum_{n=0}^{N} i^n \, j_n\big(k\|\boldsymbol{x}\|\big) \sum_{m=-n}^{n} \alpha_n^m \, Y_n^m(\widehat{\boldsymbol{x}}), \tag{39}$$

where for $N = \lceil \pi \, R \, e \, / \, \lambda \rceil + \Delta$ and the normalized absolute truncation error is bounded as

$$\varepsilon_N(\boldsymbol{x}) \leqslant \sum_{n>N} (2n+1) \big| j_n\big(k\|\boldsymbol{x}\|\big) \big| \tag{40a}$$

$$\leq \sqrt{\pi} \sum_{n>N} \frac{\big(\pi\|\boldsymbol{x}\|/\lambda\big)^n}{\Gamma(n+1/2)} \leqslant \upsilon \, e^{-\Delta}, \tag{40b}$$

where $\upsilon \approx 0.67848$ and $\Gamma(\cdot)$ is the Gamma function. The proof is structurally similar to the proof of Theorem 1 and hinges on the asymptotically decaying behavior of spherical Bessel functions in (40a) and (40b). More details about characterization of 3D multipath fields can be found in [27].

We note that by truncating $F(\boldsymbol{x})$ to N terms in (39), the number of significant $\{\alpha_n^m\}$ coefficients is $(N+1)^2$. Hence, we can assert:

***Definition** 2 (**Dimensionality of 3D Multipath Fields**):* For a spherical region in space given by $\|\boldsymbol{x}\| \leqslant R$, the maximum dimensionality of well-modeled 3D multipath is given by

$$\mathcal{D}_R^{\text{3D}} \triangleq \left(\lceil e\,\pi\,R/\lambda\rceil + 1\right)^2 \approx 72.923\,(R/\lambda)^2. \tag{41}$$

In summary, $\mathcal{D}_R^{\text{3D}}$ given in (41) *bounds* the spatial dimensionality of 3D multipath and increases quadratically with R/λ, not with the volume of the region. For the sphere, the dimensionality scales with the surface area. It is sufficient to use only $\mathcal{D}_R^{\text{3D}}$ of α_n^m in (36) to effectively encode any field within a distance R of the origin.

IV. Karhunen-Loeve Expansion of Random Multipath Fields: Multipath Richness

In Section III, we found an upper bound on the MSE of multipath field truncation error when the field is represented by the natural choice of orthonormal basis in (11). We showed that the essential dimensionality of 2D multipath, which is observed in a disk with radius R, is $2N+1 = 2\lceil \pi\, R\, e\,/\,\lambda\rceil + 1$, regardless of stochastic scattering characteristics. Since accurate truncation of multipath to $2N+1$ terms applies for any (and every) multipath far-field, $2N+1$ serves as an upper bound for multipath dimensionality. But, does $2N+1$ truly predict the dimensionality of a random multipath field with a specific spatial correlation function (SCF)? Of particular interest is the case where multipath power has a limited angular range. It is generally known that a limited angle of arrival makes the multipath process correlated and hence, reduces its degrees of freedom. However, quantification of the relation between angular power range and multipath dimensionality, which is based on the general wave propagation and stochastic scattering theory, deserves further investigation.

The treatment of multipath fields using the orthonormal basis in (11) is insufficient for analyzing the effects of limited angular power range on multipath dimensionality. In fact, $\{\alpha_n\}_{n\in\mathbb{Z}}$ that encode multipath in (11) are correlated random variables, as defined in (12)-(19). While multipath truncation to $2N+1$ terms in Section III is universally applicable to any multipath field, regardless of correlation in $\{\alpha_n\}_{n\in\mathbb{Z}}$, a customized model should allow the *optimal*, maximally parsimonious representation of a particular field with a given SCF. With a fixed truncation length, the truncation error will be minimum when the multipath field is truncated in its optimal representation, or the MMSE truncation. Alternatively, with a fixed truncation error, the optimal modeling of multipath

allows the minimum truncation length. For 2D fields with a limited angular power range, multipath dimensionality will be often much less than the predicted $2N+1$.

In this section, we first define the optimal representation of random multipath fields and then, use it to quantify the notion of multipath richness. The Karhunen-Loeve (KL) expansion is a widely-used signal processing model for the optimal representation of stochastic processes in time domain. The KL expansion takes away the redundant correlation of a random process and allows its representation with the minimum number of uncorrelated terms [14]. Here, we apply the KL expansion for the representation of stochastic multipath fields in spatial domain. The objective is to find the maximally parsimonious truncation of a random field $F(\boldsymbol{x})$ and the effects of limited angular power range on multipath dimensionality. The KL modeling of multipath is a novel means of defining multipath richness that complements and confirms previous approaches in [10], [12].

Based on the KL theory, the optimal expansion of a random multipath field $F(\boldsymbol{x})$ in the region $\|\boldsymbol{x}\| \leqslant R$ may be written as

$$F(\boldsymbol{x}) = \sum_{n=0}^{+\infty} \sqrt{\lambda_n}\, \beta_n\, \Psi_n(\boldsymbol{x}), \tag{42}$$

where β_n is a sequence of uncorrelated (white) random variables with unit variance, and $\lambda_n \geqslant 0$ and $\Psi_n(\boldsymbol{x})$ are the n^{th} eigenvalue and eigenfunction of the SCF, respectively. That is, in the 2D case

$$\int_0^R \int_0^{2\pi} \rho(\boldsymbol{x}_2 - \boldsymbol{x}_1)\Psi_n(\boldsymbol{x}_1) r_1 dr_1 d\varphi_1 = \lambda_n \Psi_n(\boldsymbol{x}_2), \tag{43}$$

where $\rho(\boldsymbol{x}_2 - \boldsymbol{x}_1)$ was given in (18) and $\boldsymbol{x}_1 \equiv (r_1, \varphi_1)$.

The major difference between the orthogonal representations of the random multipath field in (11) and in (42) is that the coefficients α_n (11), regarded as random variables, may be correlated with covariance coefficients given in (14), whereas all correlation is taken away from β_n in (42). Moreover, the orthonormal functions $\Psi_n(\boldsymbol{x})$ in the KL expansion (42) are customized for a particular multipath field with a given SCF, whereas the closed-form, orthonormal functions $\Phi_n(\boldsymbol{x})$ in the expansion (11) are universally applicable for any multipath field. While the universal expansion of the 2D field in (11) predicts a universal dimensionality of $2N+1$, a specific multipath richness is predictable using the KL expansion. If we assume that (42) is arranged in descending order of eigenvalues, then the truncation of multipath field $F(\boldsymbol{x})$ to $2N+1$ terms in (42) results in the MMSE [14] that is already upper bounded by the MSE in Theorem 2 for $N \geqslant \lceil e\pi R/\lambda \rceil$.

For isotropic scattering, with the APS given by $P(\varphi) = 1/2\pi, \quad \varphi \in [0, 2\pi)$, $\gamma_0 = 1$, and $\gamma_n = 0$ for $n \neq 0$, the coefficients $\{\alpha_n\}_{n\in\mathbb{Z}}$ in (11) are already uncorrelated. Therefore, $\Phi_n(\boldsymbol{x}_1)$ in (8) is the n^{th} SCF eigenfunction and $\lambda_n = 2\pi\mathcal{J}_n(R)$ is its corresponding eigenvalue. In other words, the truncation MSE bound in Theorem 2 is tight for an isotropic multipath field, asserting it as the richest type of scattering.

For other types of scattering and according to (42), the number of effective terms that generates the field is directly related to the eigenvalue spread of SCF. Therefore, we study the characteristic of SCF eigenvalues. In Section IV-A, we define multipath richness based on SCF eigenvalues and also prove a lower bound on the maximum eigenvalue of $\rho(\boldsymbol{x}_2 - \boldsymbol{x}_1)$. In Section IV-B, we provide a systematic numerical method to calculate SCF eigenvalues. Section IV-C presents numerical results and compares the defined multipath richness in Section IV-A with those provided in [12].

A. Multipath Richness

We first review some of the important properties of SCF eigenvalues. The integral operator A with kernel $\rho(\boldsymbol{x}_2 - \boldsymbol{x}_1)$

$$Af \triangleq \int_0^R \int_0^{2\pi} \rho(\boldsymbol{x}_2 - \boldsymbol{x}_1)\, f(\boldsymbol{x}_1) r_1 dr_1 d\varphi_1 \tag{44}$$

is symmetric, self-adjoint and compact [15]. Consequently, the set of non-zero eigenvalues of $\rho(\boldsymbol{x}_2 - \boldsymbol{x}_1)$ has either a finite cardinality or, if there are infinitely many eigenvalues, their limit is zero [15, p. 191]. We now show that the sum of all the eigenvalues of the kernel $\rho(\boldsymbol{x}_2 - \boldsymbol{x}_1)$ is finite and equal to πR^2, which is also equal to the total normalized multipath energy in a 2D disk of radius R. From [28, pp 117-118], it is known that the sum of eigenvalues is equal to the trace of kernel

$$\sum_n \lambda_n = \int_0^R \int_0^{2\pi} \rho(\boldsymbol{x}_1 - \boldsymbol{x}_1) r_1 dr_1 d\varphi_1 = \pi R^2, \tag{45}$$

since $\rho(\boldsymbol{x}_1 - \boldsymbol{x}_1) = \rho(0) = 1$ according to (12) and (17).

Now we are in a position to define multipath richness from the characteristics of SCF eigenvalues. In defining multipath richness, we use the fact that the total sum of eigenvalues in (42) is finite and propose the notion of significant eigenvalues.

***Definition** 3 (**Multipath Richness**): Suppose that in the KL expansion of multipath field $F(\boldsymbol{x})$ given by* (42) *the eigenvalues are indexed in descending order (including multiple eigenvalues).*

The field is said to have richness M when the following normalized eigenvalue residual is less than 0.01.

$$\frac{\sum_{m>M}\lambda_m}{\sum_m \lambda_m} < 0.01. \tag{46}$$

In other words, multipath richness is defined to be M when at least 99% of the multipath energy is contained in the first M eigenvalues.

Now, we wish to study the properties of eigenvalues for multipath fields with a limited angular spread in the APS. To this end, we assume the APS, $P(\varphi)$ in (12), to be uniformly distributed in the azimuth angular interval $\varphi \in [-\Omega, \Omega)$, where Ω is a fraction of π. We denote this fraction by $\Omega = \pi/\tau$ ($\tau > 1$). In short, we refer to the directional APS as $P_\Omega(\varphi) = 1/2\Omega$.

The following theorem proves a lower bound on the largest eigenvalue of the SCF. It is noted that, according to (45), the sum of eigenvalues is fixed for a given disk radius R. Therefore, a lower bound on the largest eigenvalue upper bounds the sum of remaining eigenvalues. Hence, according to Definition 3, a larger lower bound on the maximum eigenvalue means reduced multipath richness.

***Theorem** 3 (**A Lower Bound on the Largest Eigenvalue of the Spatial Correlation Function**): The largest eigenvalue of the spatial correlation function in* (17) *in a 2D disk of size R with a uniformly directional APS $P_\Omega(\varphi)$ in the range $\varphi \in [-\Omega, \Omega)$, where $\Omega = \pi/\tau$, $\tau > 1$, is lower bounded by*

$$\lambda_{\max} \geqslant \max_{q\in\mathbb{Z}} \Big\{ 2\pi \sum_m \mathcal{J}_m(R)\,\mathrm{sinc}^2(m\Omega - q\pi) \Big\}. \tag{47}$$

□

The proof is provided in Appendix III. It may be verified that the lower bound on the maximum eigenvalue increases with decreasing the APS range Ω. This, in turn, results in a smaller multipath eigenvalue spread. Therefore, (47) quantifies, to some extent, the well-known qualitative relationship between eigenvalue spread and multipath richness. Equation (47) is useful in most situations, where closed-form expressions for multipath SCF eigenvalues do not exist.

Before concluding this section, we review a standard upper bound on the largest eigenvalue. For the 2D case, the upper bound is written as [15, p. 86]

$$\lambda_{\max} = \|\rho(\boldsymbol{x}_2 - \boldsymbol{x}_1)\| \leqslant \left[\int_0^R \int_0^R \int_0^{2\pi} \int_0^{2\pi} \big|\rho(\boldsymbol{x}_2 - \boldsymbol{x}_1)\big|^2 d\varphi_1 d\varphi_2 r_1 dr_1 r_2 dr_2 \right]^{1/2}, \tag{48}$$

which, by using the definition of $\rho(\boldsymbol{x}_2 - \boldsymbol{x}_1)$ in (18), is simplified to

$$\lambda_{\max} \leqslant 2\pi \sqrt{\sum_m \mathcal{J}_m(R) \sum_n \mathcal{J}_n(R) |\gamma_{n-m}|^2}. \tag{49}$$

In Section IV-C, the numerical comparison of the largest SCF eigenvalue with the lower and upper bounds shows that the derived lower bound in (47) is quite close to the actual largest eigenvalue.

B. A Systematic Numerical Method for Eigenvalue Calculation

Numerical calculation of SCF eigenvalues is often inevitable, because closed-form expressions for SCF eigenvalues may not exist. More specifically, one needs to numerically solve (43), which is also known as the Fredholm equation [15, p. 209]. A known technique to solve equations similar to (43) is to accurately approximate the integrals on the left hand side by a sum, and transform the problem to a finite-dimension, matrix-based eigenequation [16, pp. 782-785]. For this purpose, a set of P quadrature points and quadrature weights are required to sufficiently *sample* the integral. Suppose that the q^{th} quadrature point and quadrature weight are denoted by $\boldsymbol{x}_q$ and w_q, respectively. Then, at each point $\boldsymbol{x}_q$, (43) is approximated as

$$\sum_{p=0}^{P-1} w_p \rho(\boldsymbol{x}_q - \boldsymbol{x}_p) \Psi_n(\boldsymbol{x}_p) = \lambda_n \Psi_n(\boldsymbol{x}_q). \tag{50}$$

The computational complexity of simultaneously solving P equations of the form (50) is $O(P^3)$ [16, p. 783]. Hence, a clever choice of quadrature points and weights is required to optimally sample the region of interest. As can be seen from (43), this involves selection of P points in a 2D circular region (or 3D spherical region for 3D multipath). For a large region radius R, populating the area (or volume) with enough quadrature points becomes problematic (as a rule of thumb, points at the outer edges of the region should be sampled with the separation of around $\lambda/2$).

In this section, we define an alternative approach for the numerical solution of SCF eigenvalues, which is based on the equivalence of representations of multipath field $F(\boldsymbol{x})$ in (11) and (42). The main advantage of the proposed algorithm over the aforementioned quadrature-based numerical technique is that it does not try to explicitly solve (43), and as such, the selection of quadrature

points is avoided. To see this, we combine (11) and (42) to write

$$F(\boldsymbol{x}) = \sum_{n=-\infty}^{+\infty} \sqrt{2\pi \mathcal{J}_n(R)}\alpha_n \Phi_n(\boldsymbol{x}) = \sum_{n=0}^{+\infty} \sqrt{\lambda_n}\beta_n \Psi_n(\boldsymbol{x}). \tag{51}$$

It is evident from (51) that the change of orthonormal basis from $\Phi_n(\boldsymbol{x})$ to $\Psi_n(\boldsymbol{x})$ *whitens* the weighted random sequence $\sqrt{2\pi \mathcal{J}_n(R)}\alpha_n$ to obtain the uncorrelated random sequence $\sqrt{\lambda_n}\beta_n$ with variance λ_n. Let the covariance matrix of the sequence $\sqrt{2\pi \mathcal{J}_n(R)}\alpha_n$ be denoted by $\mathbf{\Gamma}$ with elements at the m^{th} row and n^{th} column given by $\mathcal{E}\{\sqrt{2\pi \mathcal{J}_m(R)}\alpha_m . \sqrt{2\pi \mathcal{J}_n(R)}\alpha_n^*\} = 2\pi\sqrt{\mathcal{J}_m(R)\mathcal{J}_n(R)}\gamma_{m-n}$. From [29], we know that the diagonalization of the covariance matrix $\mathbf{\Gamma}$

$$\mathbf{Q\Gamma Q}^H = \mathbf{D} \tag{52}$$

transforms correlated random variables $\sqrt{2\pi \mathcal{J}_n(R)}\alpha_n$ into uncorrelated random variables $\sqrt{\lambda_n}\beta_n$, where $\mathbf{Q}$ is the eigenmatrix of $\mathbf{\Gamma}$, $\mathbf{D}$ is the diagonal eigenvalue matrix with the n^{th} diagonal element equal to λ_n, and superscript H denotes Hermitian transpose. In Section III, we concluded that the first $2N+1$ terms of $\sqrt{2\pi \mathcal{J}_n(R)}\alpha_n$ adequately represent the field. We summarize the above discussion in the following algorithm to numerically obtain SCF eigenvalues, λ_n.

Algorithm 1 - Systematic Numerical Calculation of λ_n:

1) *Based on Theorem 1 and Theorem 2, truncate the random sequence $\sqrt{2\pi \mathcal{J}_n(R)}\alpha_n$ in (51) with truncation length $N \geqslant \lceil e\pi R\lambda \rceil$, to obtain the random vector*

$$\mathbf{v} = \begin{bmatrix} \sqrt{2\pi \mathcal{J}_{-N}(R)}\alpha_{-N} & \cdots & \sqrt{2\pi \mathcal{J}_N(R)}\alpha_N \end{bmatrix}^T .$$

2) *Using* (14)*, form the covariance matrix for the random vector* $\mathbf{v}$ *defined as* $\mathbf{\Gamma}_{2N+1} = \mathcal{E}\{\mathbf{v}\mathbf{v}^H\}$.

3) *The eigenvalues of the covariance matrix* $\mathbf{\Gamma}_{2N+1}$ *give the first* $2N+1$ *eigenvalues of the SCF* $\rho(\boldsymbol{x}_2 - \boldsymbol{x}_1)$.

C. Eigenvalue Analysis

First, we present the lower bound, upper bound, and numerical results for the SCF largest eigenvalue for a set of directional scatterers. The results are shown in Fig. 2. The parameter is the APS range Ω, which varies from $\Omega/\pi = 1/20$ (highly directional) to $\Omega/\pi = 1$ (isotropic). The

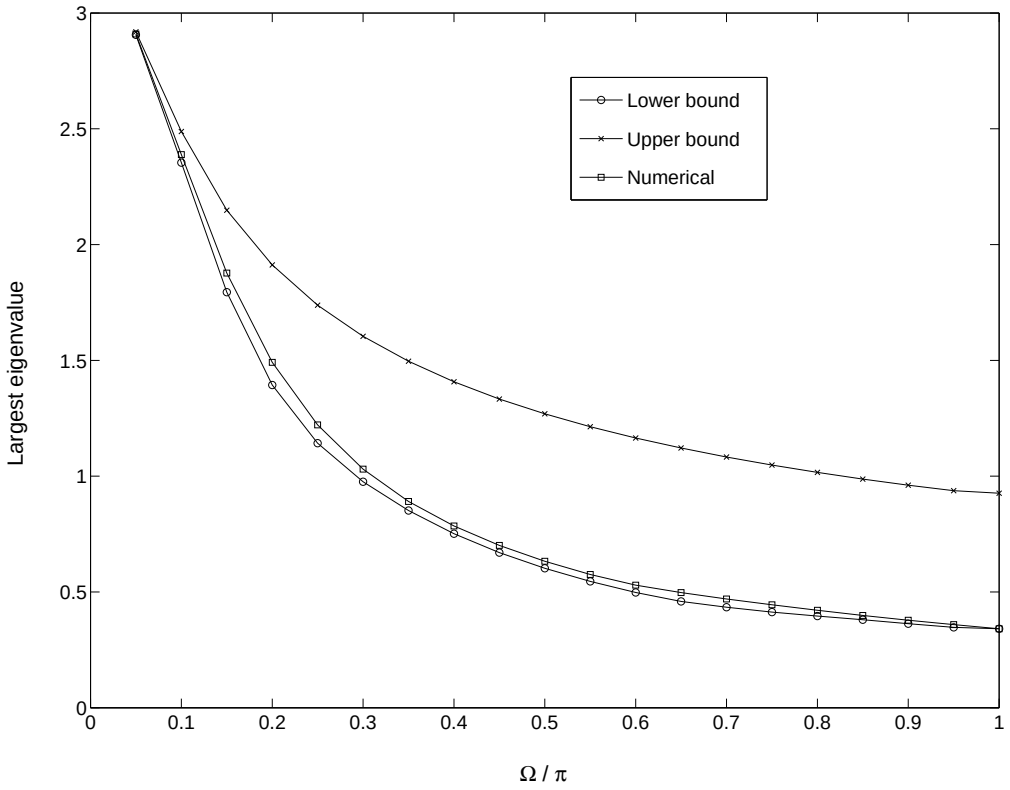

Fig. 2. The largest eigenvalue of the spatial correlation function as a function of APS range Ω. The eigenvalues are computed on a disk of radius $R = 1\,\lambda$. The lower bound is computed using (47) in Theorem 3. The upper bound is computed using (49). Also in the figure, the largest eigenvalue is calculated numerically using Algorithm 1 in Section IV-B. The results show that the lower bound is very close to the actual eigenvalue and that multipath richness reduces with reducing Ω. (Also see Table I.)

eigenvalues are computed on a disk with radius $R = 1\,\lambda$. The lower bound is computed using (47) in Theorem 3. The upper bound is computed using (49). Also in the figure, the largest eigenvalue is calculated numerically using Algorithm 1, which was described in Section IV-B. It is clear from this figure that the proposed lower bound on the largest eigenvalue is much closer to the actual eigenvalue than the upper bound and provides very good estimates of the largest SCF eigenvalue. As the APS range Ω becomes smaller, the largest eigenvalue increases and multipath richness is reduced. Multipath richness for some typical values of Ω in this figure are calculated according to Definition 3 and given in Table I. The results quantitatively confirm the qualitative speculations that reducing multipath angular power spread would make the field more spatially correlated and reduce its *richness*.

TABLE I

DIMENSION OR RICHNESS OF MULTIPATH FIELDS STUDIED IN FIG. 2-3, WHICH IS CALCULATED USING DEFINITION 3 AND ITS COMPARISON WITH (53) [12].

APS range Ω/π	0.05	0.25	0.5	0.75	1
Definition 3	3	6	9	12	15
$2\lceil \frac{\Omega\, e\, R}{\lambda} \rceil + 1$	3	7	11	15	19

Next, we present the numerical analysis of eigenvalues for three different APS's with angular spread $\Omega/\pi = 0.05, 0.5$, and 1. The eigenvalues are computed on a disk of size $R = 1\,\lambda$ using Algorithm 1 in Section IV-B. The results are shown in Fig. 3. From this figure it is clear that the eigenvalue spread decreases with decreasing the APS range Ω. Table I shows the predicted dimension or richness of multipath fields in Fig. 3 according to Definition 3, where the eigenvalue residual falls below 0.01 of the total πR^2. For comparison, we have also presented the predicted dimension of directional multipath fields in [12]. It was argued in [12] that the dimension of spatial multipath fields with a restricted angle of arrival between $[-\Omega, \Omega)$ in a 2D region of size R is equal to

$$2M' + 1, \quad M' = \left\lceil \frac{\Omega\, e\, R}{\lambda} \right\rceil. \tag{53}$$

Compared to (35), the above dimension takes the restricted APS range Ω into account. From Table I it is observed that the calculated richness using Definition 3 is either identical to or below the predicted dimension in (53).

V. CONCLUSIONS

The degree to which multipath fields are resolvable in space depends on the size of space where the field is coupled to. For 2D spatial regions of radius R, we proved that the number of effective multipath modes is limited by $2N + 1$, where $N = \lceil \pi e R/\lambda \rceil$. For 3D spatial regions of radius R, the number of effective multipath modes is limited by $(N+1)^2$. We also defined random multipath richness based on the number of SCF eigenvalues in the KL expansion that captures 99% of the multipath energy. We showed that multipath richness is upper bounded by $2N + 1$ in the MMSE sense and the bound is achieved for isotropic multipath. By proving a lower bound on the largest

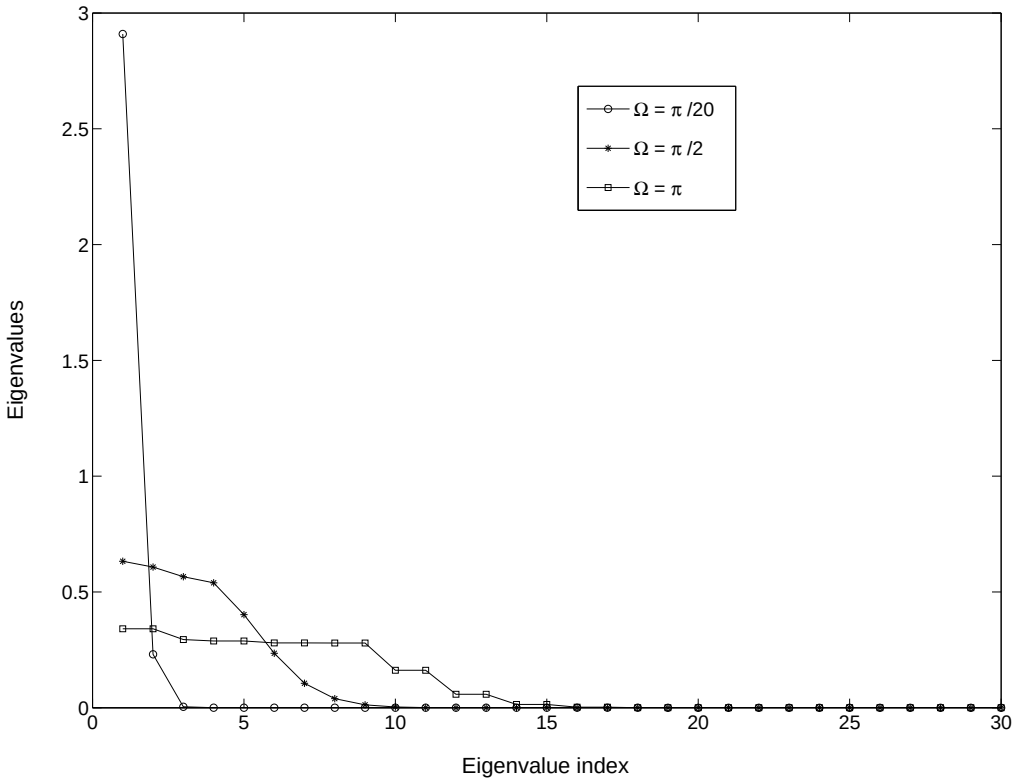

Fig. 3. Numerical eigenvalue analysis for three different APS's with the range $\Omega/\pi = 0.05, 0.5$, and 1. The eigenvalues are computed on a disk of radius $R = 1\,\lambda$ using Algorithm 1 in Section IV-B. The eigenvalue spread decreases with decreasing Ω.

SCF eigenvalue, we quantitatively verified the well-known reduction of multipath richness with reducing the APS angular range.

APPENDIX I
PROOF OF THEOREM 1

Proof: For reference, (25) is repeated by defining $z \triangleq \pi\|\boldsymbol{x}\|/\lambda$ and hence, $kr = 2\pi/\lambda\|\boldsymbol{x}\| = 2z$

$$\zeta_N(\boldsymbol{x}) \;\leqslant\; 2\sum_{n>N}|J_n(2z)| \leqslant 2\sum_{n>N}\frac{z^n}{n!} \triangleq 2\,R_N(z). \tag{54}$$

Therefore, we find an upper bound on $R_N(z)$, which is expanded by changing the summation variable as

$$R_N(z) = \sum_{n>N} \frac{z^n}{n!} = \exp(z) - \sum_{n=0}^{N} \frac{z^n}{n!} \tag{55a}$$

$$= \frac{z^{N+1}}{(N+1)!}\Big(\sum_{n=0}^{\infty} \frac{(N+1)!}{(N+1+n)!} z^n\Big). \tag{55b}$$

Note that for integer $n \geqslant 0$ each term in the summation in (55b) is upper bounded as

$$\frac{(N+1)!}{(N+1+n)!} z^n \leqslant \Big(\frac{z}{N+2}\Big)^n. \tag{56}$$

Hence, for integer $N \geqslant 0$ satisfying $N > z-2$, we can use the sum of geometric series to upper bound $R_N(z)$ in (55b) as

$$R_N(z) \leqslant \frac{z^{N+1}}{(N+1)!}\Big(\frac{N+2}{N+2-z}\Big). \tag{57}$$

Now, we use the Stirling lower bound, $n! > \sqrt{2\pi n}\, n^n\, e^{-n}$, to write

$$\frac{z^{N+1}}{(N+1)!} \leqslant \frac{1}{\sqrt{2\pi(N+1)}}\Big(\frac{e\,z}{N+1}\Big)^{N+1}. \tag{58}$$

Now, using the following exponential inequality

$$\Big(\frac{e\,z}{N+1}\Big)^{N+1} = \Big(1 + \frac{e\,z - N - 1}{N+1}\Big)^{(N+1)} \leqslant e^{ez-N-1}, \tag{59}$$

we obtain the following upper bound on $R_N(z)$

$$R_N(z) \leqslant \frac{e^{ez-N-1}}{\sqrt{2\pi(N+1)}}\Big(\frac{N+2}{N+2-z}\Big). \tag{60}$$

To contain the exponential in (60), for a given z, consider selecting $N(z) = \lceil ez \rceil$. Then,

$$e\,z \;\leqslant\; N(z) < e\,z \,+\, 1, \tag{61}$$

from which it can be shown

$$\Big(\frac{N(z)+2}{N(z)+2-z}\Big) \leqslant \frac{e}{e-1} = 1.58197... \tag{62a}$$

$$\exp(e\,z - N(z) - 1) \leqslant 1/e = 0.36787...\ . \tag{62b}$$

Using (62a) and (62b) in (60) yields

$$R_{N(z)}(z) \leqslant \frac{1}{(e-1)\sqrt{2\pi(N(z)+1)}} = \frac{0.23217...}{\sqrt{N(z)+1}}. \tag{63}$$

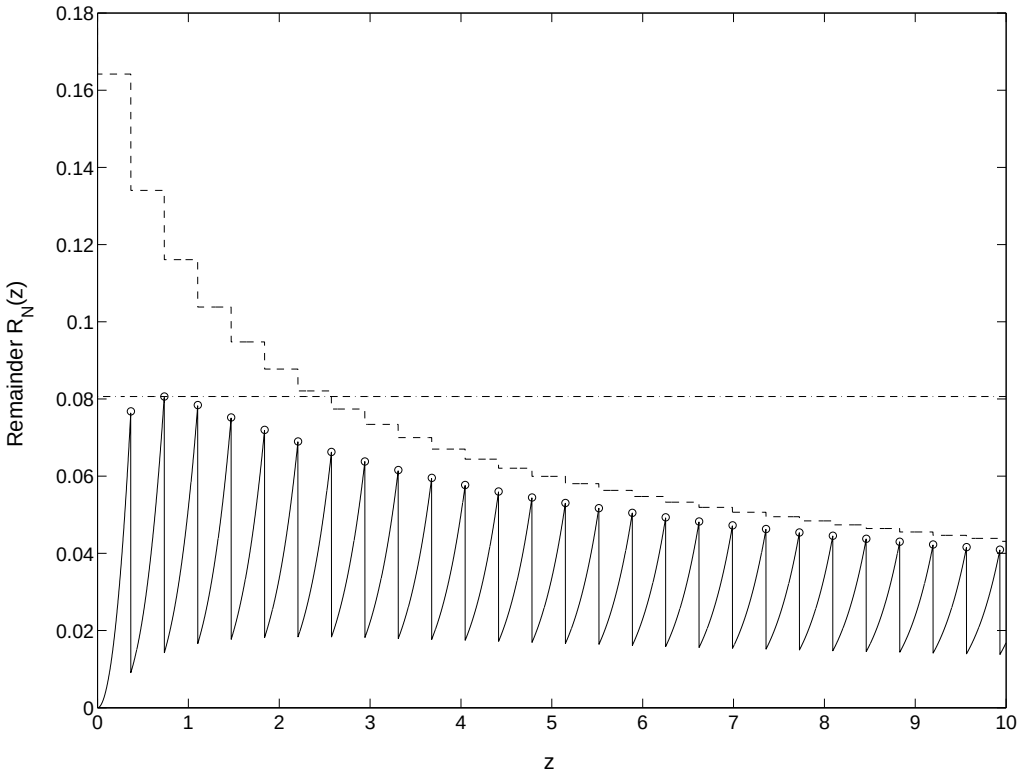

Fig. 4. The remainder $R_N(z)$ in (55a) with $N = N(z) \equiv \lceil e\, z \rceil$. The stepped curve is the bound given by (63) and the uniform bound corresponds to (64).

Selecting $N(z) = \lceil ez \rceil$ implies that $R_{N(z)}(z)$ in (63) is piecewise function of z with local maxima at $z \in \{1/e, 2/e, 3/e, \ldots\}$, where $N(z)$ steps up to the next integer value. By searching over these local maxima we can use the exact expression (55a) to obtain a uniform tight bound:

$$\begin{aligned} R_{N(z)}(z) &\leqslant \max_N R_N(N/e) = R_2(2/e) \\ &= \exp\left(\frac{2}{e}\right) - \left(1 + \frac{2}{e} + \frac{2}{e^2}\right) = 0.080635... \end{aligned} \tag{64}$$

which improves on (63) when $N(z) \leq 7$. Fig. 4 displays the truncation error bounds for $R_N(z)$ given in (63) and (64) as a function of z and using $N = \lceil e\, z \rceil$.

When $N \geqslant N(z)$, which we refer to as the *critical regime*, we infer from (64) that $R_N(z) \leq 0.080635....$ Therefore, $\zeta_N(\boldsymbol{x}) \leq 0.16127$ that establishes (26) for $\Delta = 0$.

Now, we show that $R_N(z)$, for a fixed z, exponentially decreases as N increases provided that $N > z - 2$. First, we note that for a positive fixed z, $R_N(z)$ in (55a) is decreasing with N. Using

(55b) we write the ratio $R_{N+\Delta}(z)/R_N(z)$ for $\Delta \geqslant 0$ as

$$\frac{R_{N+\Delta}(z)}{R_N(z)} = \frac{z^{N+\Delta+1}}{(N+\Delta+1)!}\frac{(N+1)!}{z^{N+1}}\frac{\sum_{n=0}^{\infty}\frac{(N+\Delta+1)!}{(N+\Delta+1+n)!}z^n}{\sum_{n=0}^{\infty}\frac{(N+1)!}{(N+1+n)!}z^n}. \tag{65}$$

We observe that for $\Delta \geqslant 0$

$$\frac{(N+\Delta+1)!}{(N+\Delta+1+n)!} = \frac{1}{(N+\Delta+2)\cdots(N+\Delta+1+n)} \tag{66}$$

$$\leqslant \frac{1}{(N+2)\cdots(N+1+n)} = \frac{(N+1)!}{(N+1+n)!}. \tag{67}$$

Therefore, each term in the summation in numerator in (65) is smaller than each term in the summation in the denominator and hence, the ratio is less than 1, which yields

$$\frac{R_{N+\Delta}(z)}{R_N(z)} \leqslant \frac{z^{\Delta}}{(N+2)(N+3)\cdots(N+\Delta+1)} \tag{68a}$$

$$\leqslant \Big(\frac{z}{N+2}\Big)^{\Delta} = \frac{1}{\alpha^{\Delta}}\Big|_{\alpha=(N+2)/z}. \tag{68b}$$

Therefore, whenever $N > z-2$, we have $\alpha > 1$ and the remainder $R_{N+\Delta}(z)$ decreases exponentially as Δ increases. In the critical regime, $N \geqslant \lceil ez \rceil$, this implies $\alpha > e$ and the exponential decrease is at least as fast as $\exp(-\Delta)$ by (68b). Therefore, the truncation error upper bound for $N+\Delta = \lceil ez \rceil + \Delta$ is written as

$$\zeta_{N+\Delta}(\boldsymbol{x}) \leqslant 2\,R_{N+\Delta}(z) \leqslant 2\,R_N(z)\,e^{-\Delta} \leqslant 0.16127e^{-\Delta} \tag{69}$$

It is also easily verified that for all positive values of z satisfying

$$\frac{K-1}{e} < z \leqslant \frac{K}{e} \Rightarrow N = \lceil\, e\,z\,\rceil = K, \quad K \in \mathbb{N},$$

the inequality $N > z-2$ is automatically satisfied and the assumptions throughout the proof are valid. ■

APPENDIX II

PROOF OF THEOREM 2

Proof: The proof of Theorem 2 is similar to the proof of Theorem 1. Referring to (33) and using (24), we first find an upper bound for the summation in the integral

$$S_N(z) \triangleq \sum_{n=N+1}^{+\infty} J_n^2(2z) \leqslant \sum_{n=N+1}^{+\infty} \frac{z^{\,2n}}{(n!)^{\,2}}, \tag{70}$$

where $z \triangleq \pi\|\boldsymbol{x}\|/\lambda$. Using a similar procedure as in (55a)-(56), we obtain

$$S_N(z) \leqslant \frac{z^{\,2(N+1)}}{((N+1)!)^2}\frac{1}{1-\frac{z^2}{(N+2)^2}} \tag{71}$$

for $N+2 > z$. Now using the same steps as (58)-(59), the following bound is derived

$$S_N(z) \leqslant \frac{e^{\,2(e\,z-N-1)}}{2\pi(N+1)}\frac{1}{1-\frac{z^2}{(N+2)^2}}. \tag{72}$$

If we choose $ez \leqslant N = \lceil ez \rceil < ez+1$, we obtain

$$S_N(z) \leqslant \frac{0.0249}{(N+1)}. \tag{73}$$

We can further examine the bound on $S_N(z)$ given in (71) at critical points of the ceiling function ($z = k/e$, $k \in \mathbb{N}$) to obtain a universal upper bound

$$S_N(z) \leqslant 0.004649, \tag{74}$$

by choosing $z = 1/e$ in (71). Similar to the steps in (65)-(68b), it is possible to show that for $\Delta \geqslant 0$, $N = \lceil ez \rceil$, and $N+2 > z$, the following ratio holds

$$\frac{S_{N+\Delta}(z)}{S_N(z)} \leqslant e^{-2\Delta}. \tag{75}$$

Based on (74), it is possible to show that the truncation MSE in (33)

$$\bar{\varepsilon}_N(R) = \frac{\int_0^R 2S_N(z)\,r\,dr}{1/2\,R^2} \leqslant 0.009298. \tag{76}$$

Moreover, if we choose $N_R = \lceil e\,\pi\,R/\lambda \rceil + \Delta$, so that $S_N(z)$ at the outer edge of disc is bounded as $S_N(z) \leqslant 0.004649\,e^{-2\Delta}$, from (75) we conclude that $S_N(z) \leqslant 0.004649\,e^{-2\Delta}$ for every $r \leqslant R$. Therefore, $\bar{\varepsilon}_N(R) \leqslant 0.009298e^{-2\Delta}$, which completes the proof. ■

APPENDIX III
PROOF OF THEOREM 3

Proof: Before proceeding, we remember that according to the maximum eigenvalue property [15, p. 198] and by the definition of the operator norm [15] for the kernel $A = \rho(\boldsymbol{x}_2 - \boldsymbol{x}_1)$

$$\lambda_{\max} = \|A\| \geqslant \langle Ag, g\rangle, \quad \forall g : \|g\| = 1, \tag{77}$$

it is possible to find a lower bound on the maximum eigenvalue by arbitrarily choosing any function g with the only condition being that $\|g\| = 1$. In the following, we will obtain a close lower bound

for $\lambda_{\max}$ by proper choice of g. Let the function $g(\boldsymbol{x})$ in the region $\|\boldsymbol{x}\| \leqslant R$ and $\boldsymbol{x} \equiv (r, \varphi)$ be expanded as

$$g(\boldsymbol{x}) = \sum_{p=-\infty}^{\infty} i^p b_p \, \frac{J_p(kr)}{\sqrt{\mathcal{J}_p(R)}} \, \frac{e^{ip\varphi}}{\sqrt{2\pi}}, \tag{78}$$

where $\|g\| = 1$ requires that $\sum_p |b_p|^2 = 1$. We write the inner product $\langle Ag, g\rangle \triangleq \mu$ using (44), the definition of $\rho(\boldsymbol{x}_2 - \boldsymbol{x}_1)$ in (18), and the definition of g in (78), which yields

$$\mu = 2\pi \sum_m \sqrt{\mathcal{J}_m(R)}\, b_m \sum_n \sqrt{\mathcal{J}_n(R)}\, b_n^* \, \gamma_{n-m}. \tag{79}$$

Now, we use the definition of γ_{n-m} in (14) for a directional APS $P_\Omega(\varphi)$ to write

$$\mu = \frac{\pi}{\Omega} \int_{-\Omega}^{\Omega} \Big| \sum_m \sqrt{\mathcal{J}_m(R)}\, b_m \, e^{im\varphi} \Big|^2 \, d\varphi. \tag{80}$$

The orthonormal basis functions for the limited range $[-\Omega, \Omega) = [-\pi/\tau\,, \pi/\tau)$ are $\big\{e^{in\tau\varphi}/\sqrt{2\Omega}\big\}_{n\in\mathbb{Z}}$. We expand the exponentials in (80) in terms of the new basis functions

$$e^{im\varphi} = \sum_q \xi_{m,q} \, \frac{e^{iq\tau\varphi}}{\sqrt{2\Omega}}, \tag{81}$$

where $\xi_{m,q} \triangleq \sqrt{2\Omega}\,\mathrm{sinc}(m\Omega - q\pi)$. Replacing (81) into (80) and changing the summation order yields the following expression

$$\mu = \frac{\pi}{\Omega} \int_{-\Omega}^{\Omega} \Big| \sum_q \beta_q \, \frac{e^{iq\tau\varphi}}{\sqrt{2\Omega}} \Big|^2 \, d\varphi, \tag{82}$$

where β_q is defined as

$$\beta_q \triangleq \sum_m \sqrt{\mathcal{J}_m(R)}\, b_m \xi_{m,q}. \tag{83}$$

Now, using the orthonormality of the basis functions in (82) we write

$$\mu = \frac{\pi}{\Omega} \sum_q \beta_q^2 \tag{84}$$

Since all the terms in the summation are non-negative, the inner product μ is greater than every β_q^2 including its maximum $\beta_{\max}^2 \triangleq \max_q\{\beta_q^2\}$. That is, $\mu \geqslant \beta_{\max}^2$. To find the closest lower bound on μ, we first use Cauchy's inequality to upper bound each term β_q^2 in (83)

$$\beta_q^2 = \Big| \sum_m \sqrt{\mathcal{J}_m(R)}\, b_m \xi_{m,q} \Big|^2 \leqslant \Big(\sum_m \mathcal{J}_m(R) \xi_{m,q}^2 \Big) \Big(\sum_m b_m^2 \Big), \tag{85}$$

where the upper bound is achieved when

$$b_{m,q} = c_q \sqrt{\mathcal{J}_m(R)} \xi_{m,q}, \tag{86}$$

and c_q is a constant that is chosen

$$c_q = \frac{1}{\sqrt{\sum_m \mathcal{J}_m(R)\xi_{m,q}^2}} \tag{87}$$

to normalize the function g in (78) in the region $\|\boldsymbol{x}\| \leqslant R$. Therefore, by choosing $b_{m,q}$ according to (86) each term β_q^2 is maximized as $\beta_q^2 = \sum_m \mathcal{J}_m(R)\xi_{m,q}^2$. And by definition,

$$\beta_{\max}^2 \triangleq \max_q\{\beta_q^2\} = \max_q \sum_m \mathcal{J}_m(R)\xi_{m,q}^2. \tag{88}$$

Finally, by combining (77), the definition of $\xi_{m,q}$, and (88) the following lower bound on the maximum eigenvalue is derived

$$\mu_{\max} \geqslant \mu \geqslant \beta_{\max}^2 = \max_q \Big\{2\pi \sum_m \mathcal{J}_m(R)\,\mathrm{sinc}^2(m\Omega - q\pi)\Big\}. \tag{89}$$

■

REFERENCES

[1] T. S. Rappaport, *Wireless Communications, Principles and Practice*, 2nd ed. Upper Saddle River: Prentice Hall, 2002.

[2] R. Kohno, "Spatial and Temporal Communication Theory Using Adaptive Antenna Array," *IEEE Personal Commun. Mag.*, vol. 5, no. 1, pp. 28–35, Feb. 1998.

[3] I. E. Telatar, "Capacity of multiple-antenna Gaussian channels," *Eur. Trans. Telecom.*, vol. 10, pp. 585–595, Nov. 1999.

[4] G. J. Foschini and M. J. Gans, "On the limits of wireless communications in a fading environment when using multiple antennas," *Wireless Personal Communications*, vol. 6, no. 2, pp. 311–355, 1998.

[5] J. P. Kermoal, P. E. Mogensen, S. H. Jensen, J. B. Andersen, F. Frederiksen, T. B. Sørensen, and K. I. Pedersen, "Experimental Investigation of Multipath Richness for Multi-Element Transmit and Receive Antenna Arrays," in *Proceedings of IEEE Vehicular conference, VTC-2000, Spring*, vol. 3, May 2000, pp. 2004–2008.

[6] A. Lozano and C. Papadias, "Layered Space-Time Receivers for Frequency-Selective Wireless Channels," *IEEE Trans. Commun.*, vol. 50, no. 1, pp. 65–73, Jan. 2002.

[7] P. W. Wolniansky, G. J. Foschini, G. D. Golden, and R. A. Valenzuela, "V-BLAST: an Architecture for Realizing Very High Data Rates over the Rich-Scattering Wireless Channel," in *URSI Int. Symp. Sig. Sys. and Elec.*, Sept.-Oct. 1998, pp. 295–300.

[8] H. M. Jones, R. A. Kennedy, and T. D. Abahayapala, "On dimensionality of multipath fileds: spatial extent and richness," in *Proc. IEEE Int. Conf. Acoustics, Speech and Signal Processing (ICASSP)*, 2002, pp. 2837–2840.

[9] R. A. Kennedy and T. D. Abhayapala, "Spatial concentration of wave-fields: towards spatial information content in arbitrary multipath scattering," in *Proc. 4th Australian Communications Theory Workshop, AusCTW'2003*, Feb. 2003, pp. 38–45.

[10] A. S. Y. Poon, R. W. Broderson, and D. N. C. Tse, "Degrees of freedom in multiple-antenna channels: a signal space approach," *IEEE Trans. Inform. Theory*, vol. 51, no. 2, pp. 523–536, Feb. 2005.

[11] D. Colton and R. Kress, *Inverse Acoustic and Electromagnetic Scattering Theory*, 2nd ed. Springer-Verlag, 1998.

[12] G. Dickins, M. Williams, and L. W. Hanlen, "On the dimensionality of spatial fields with restricted angle of arrival," in *Proc. IEEE Int. Symp. on Inform. Theory (ISIT)*, Adelaide, Australia, Sept. 2005, pp. 1033–1037.

[13] P. S. Teal, T. D. Abahayapala, and R. A. Kennedy, "Spatial correlation for general distribution of scatteres," *IEEE Signal Processing Lett.*, vol. 9, no. 10, pp. 305–308, Oct. 2002.

[14] R. G. Ghanem and P. D. Spanos, *Stochastic Finite Elements: A Spectral Approach*. Courier Dover Publications, 2003.

[15] G. Helmberg, *Introduction to Spectral Theory in Hilbert Space*. Amsterdam: North-Holland, 1969.

[16] W. H. Press, B. P. Flannery, S. A. Teukolsky, and W. T. Vetterling, *Numerical Recipes in C*. Cambridge Univeristy Press, 1992.

[17] T. Trump and B. Ottersten, "Estimation of nominal direction of arrival and angular spread using an array of sensors," *Signal Processing*, vol. 50, no. 1-2, pp. 57–69, 1996.

[18] S. Valaee, B. Champagne, and P. Kabal, "On Performance Analysis for Signaling on Correlated Fading Channels," *IEEE Trans. Signal Processing*, vol. 43, no. 9, pp. 2144–2153, Sept. 1995.

[19] M. Bengtsson and B. Ottersten, "Low-Complexity Estimators for Distributed Sources," *IEEE Trans. Signal Processing*, vol. 48, no. 8, pp. 2185–2194, Aug. 2000.

[20] B. H. Fleury, "First- and second-order characterization of direction dispersion and space selectivity in the radio channel," *IEEE Trans. Inform. Theory*, vol. 46, no. 6, pp. 2027–2044, Sept. 2000.

[21] P. A. Bello, "Characterization of randomly time-variant linear channels," *IEEE Trans. Commun. Syst.*, vol. CS-11, pp. 360–393, Dec. 1963.

[22] N. W. McLachlan, *Bessel Functions for Engineers*, 2nd ed. London: Oxford University Press, 1961.

[23] C. A. Coulson and A. Jeffrey, *Waves: A Mathematical Approach to the Common Types of Wave Motion*, 2nd ed. London: Longman, 1977.

[24] I. S. Gradshteyn and I. M. Ryzhik, *Table of Integrals, Series, and Products*, 6th ed. San Diego: Academic Press, 2000.

[25] T. Betlehem and T. D. Abhayapala, "Spatial correlation for correlated scatterers," in *Proc. IEEE Int. Conf. Acoustics, Speech, and Signal Processing (ICASSP)*, Toulouse, France, May 2006, accepted for publication.

[26] M. Abramowitz and I. A. Stegun, *Handbook of Mathematical Functions*, 10th ed. New York: Dover, 1974.

[27] T. D. Abhayapala, T. S. Pollock, and R. A. Kennedy, "Characterization of 3D spatial wireless channels," in *Proc. IEEE Veh. Technol. Conf. (VTC)*, Orlando, USA, Oct. 2003, pp. 123–127.

[28] A. V. Balakrishnan, *Applied Functional Analysis*. New York: Springer-Verlag, 1976.

[29] J. G. Proakis, *Digital Communications*, forth ed. New York: Mc Graw Hill, 2000.